

The University of Bradford Institutional Repository

<http://bradscholars.brad.ac.uk>

This work is made available online in accordance with publisher policies. Please refer to the repository record for this item and our Policy Document available from the repository home page for further information.

To see the final version of this work please visit the publisher's website. Available access to the published online version may require a subscription.

Link to publisher's version: <https://doi.org/10.1016/j.ophtha.2016.12.016>

Citation: McKendrick AM, Denniss J, Wang YX, Jonas JB and Turpin A (2017) The proportion of individuals likely to benefit from customized optic nerve head structure–function mapping. *Ophthalmology*. 124(4): 554–561.

Copyright statement: © 2017 Elsevier. Reproduced in accordance with the publisher's self-archiving policy. This manuscript version is made available under the CC–BY–NC–ND 4.0 license.



1
2
3
4
5
6
7
8
9
10
11
12
13
14
15
16
17
18
19
20
21
22

The proportion of individuals likely to benefit from customized optic nerve head structure-function mapping.

Allison M McKendrick, PhD (1), Jonathan Denniss, PhD (1,2,3), Ya Xing Wang, MD (4),
Jost B. Jonas, MD (4,5), Andrew Turpin, PhD (2)

(1) Department of Optometry & Vision Sciences, The University of Melbourne

(2) Department of Computing and Information Systems, The University of Melbourne

(3) Visual Neuroscience Group, School of Psychology, University of Nottingham, United Kingdom

(4) Beijing Institute of Ophthalmology, Beijing Tongren Eye Center, Beijing Tongren Hospital, Capital Medical University; Beijing Key Laboratory of Ophthalmology and Visual Sciences, Beijing, China

(5) Department of Ophthalmology, Medical Faculty Mannheim of the Ruprecht-Karls, University of Heidelberg, Germany

Financial Support: Australian Research Council Linkage Project 130100055 (industry partner, Heidelberg Engineering, GmbH, Germany). The funding organisation had no role in the design or conduct of this research.

Conflict of Interest: Attached forms for each author

Running Head: Who benefits from individualised structure-function mapping?

23 **Abstract:**

24 **Purpose:** Inter-individual variance in optic nerve head (ONH) position, axial length and location of
25 the temporal raphe suggest that customizing mapping between visual field locations and optic nerve
26 head sectors for individuals may be clinically useful. Here we quantify the proportion of the
27 population predicted to have structure-function mappings that markedly deviate from “average”, and
28 thus would benefit from customized mapping.

29 **Design:** Database study and case report

30 **Participants:** Population database of 2836 eyes from the Beijing Eye Study; single case report of an
31 individual with primary open angle glaucoma

32 **Methods:** Using the morphometric fundus data of the Beijing Eye Study on 2836 eyes and applying a
33 recently developed model based on axial length and ONH position relative to the fovea, we
34 determined for each measurement location in the 24-2 Humphrey visual field the proportion of eyes
35 for which, in the customized approach as compared to the generalized approach, the mapped ONH
36 sector was shifted into a different sector. We determined the proportion of eyes for which the mapped
37 ONH location was shifted by 15°, 30° or 60°.

38 **Main outcome measures:** Mapping correspondence between locations in visual field space to
39 localized sectors on the optic nerve head

40 **Results:** The largest inter-individual differences in mapping are in the nasal step region where the
41 same visual field location can map to either the superior or inferior ONH depending on other
42 anatomical features. For these visual field locations, approximately 12% of eyes showed a mapping
43 opposite to conventional expectations.

44 **Conclusions:** Anatomically customised mapping shifts the map markedly in approximately 12% of
45 the general population in the nasal step region where visual field locations can map to the opposite
46 pole of the ONH than conventionally considered. Early glaucomatous damage commonly affects this

47 region, hence individually matching structure to function may prove clinically useful for the diagnosis
48 and monitoring of progression within individuals.

49

50

51

52

53

54

55

56

57

58

59

60

61

62

63

64

65

66 **Introduction**

67 Both anatomical and functional measures are key to contemporary glaucoma diagnosis and
68 management. Typically these are measured separately, hence in order to relate these two different
69 clinical measures intelligently, it is necessary to have a mapping between the structural parameters
70 (for example, the location on the optic nerve head (ONH) or peripapillary retinal nerve fiber (RNF)
71 layer position) and locations in visual space. Different approaches to such mapping have been
72 proposed, including models derived from hand-tracing and visualisation of RNF bundle trajectories,^{1,2}
73 models derived by visualisation of the absence of RNF bundles in established glaucoma using retinal
74 photography,³ from geometrical principles,⁴⁻⁶ or from correlations between structural and functional
75 abnormalities in clinical databases.^{7,8} The advent of high resolution ocular imaging with the capacity
76 to readily and quantitatively assess ocular biometric parameters has seen an increased clinical and
77 scientific interest in the inter-individual differences in key ocular anatomical parameters that are
78 considered to contribute to this mapping.^{2, 9-11}

79 There are several key anatomical features that influence the mapping between structure and function
80 in glaucoma. These include: the position of the optic nerve head relative to the fovea; the position of
81 the temporal raphe; and axial length. While it is well established that axial length shows significant
82 variance between individuals,¹² published data on the population variance of other key parameters is
83 relatively recent. Chauhan and Burgoyne¹³ provided a histogram of the distribution of ONH positions
84 relative to the fovea in a population of 222 patients with ocular hypertension or glaucoma, and
85 showed that the position of the centre of the ONH (centre of Bruch's membrane opening) relative to
86 the fovea could differ by up to 25 degrees. A larger population distribution from the Beijing Eye
87 Study showed a distribution from 6.3° to 28.9°. ¹⁴ The temporal raphe is now directly visible using high
88 resolution OCT^{15, 16} and adaptive optics.¹⁷ The sample size of studies that have visualised and mapped
89 the raphe are relatively small (approximately 20 people), however the angle of the temporal raphe
90 appears to vary between individuals by up to 10 degrees, with an on-average positioning of
91 approximately 170 degrees from the ONH-fovea angle.^{15, 16} Variation in the position of the temporal
92 raphe has been confirmed by studies that have used lower resolution clinical OCT to look for
93 divisions between superior and inferior hemifields in macular cube data.¹⁸ The temporal raphe is a key

94 landmark dividing the superior and inferior retina and many analysis procedures for glaucoma (for
95 example: the glaucoma hemifield test¹⁹) assume a horizontal boundary between the superior and
96 inferior visual field. Hence, if the temporal raphe deviates significantly from horizontal, there is the
97 potential for very atypical mapping between visual field locations in the nasal visual field and the
98 optic nerve, and possibly misinterpretation of clinical analytics that assume a strictly horizontal divide
99 between the superior and inferior hemifields.

100 The observation of significant population variance in these key anatomical features predicts that
101 custom, personalised, mapping between structure and function might have clinical utility.^{4, 9, 15} For
102 example, personalised mapping may be important to detect early, spatially localised, signs of
103 progression (for example, mapping pointwise visual field change to sectoral change of neuroretinal
104 rim tissue or retinal nerve fiber layer); or to enable customised functional testing that is spatially
105 directed by structural abnormalities observed on OCT.²⁰ To date, while customised mapping has been
106 proposed,^{2, 4} there has been fairly limited exploration of when and for whom, it is likely to be useful.
107 Danthurebandara et al²¹ compared the strength of correlations between structure and function for
108 individually customised mapping⁴ to a commonly used population based map³ and found that
109 performance of the two mapping schema was similar. Hood et al¹¹ considered individual differences
110 in the position of the ONH relative to the fovea, and similarly found that on average, between group
111 estimates of the strength of correlation between structure and function were not improved. These
112 outcomes are hardly surprising given that most individuals within a population will have fairly
113 average anatomy and therefore the customised approach and non-customised approach will produce
114 very similar maps for many people. Consequently, when data across the population is pooled for
115 analysis, and most people are “average”, an absence of an “on-average” difference between
116 customised and non-customised mapping schema is entirely predictable. A pertinent challenge arising
117 is to identify the situations where customised mapping departs significantly from the population norm
118 and how commonly this occurs.

119 In this paper, we approach this problem by calculating the likelihood of an individual having a
120 structure-function map that significantly deviates from average, and illustrate the key anatomical

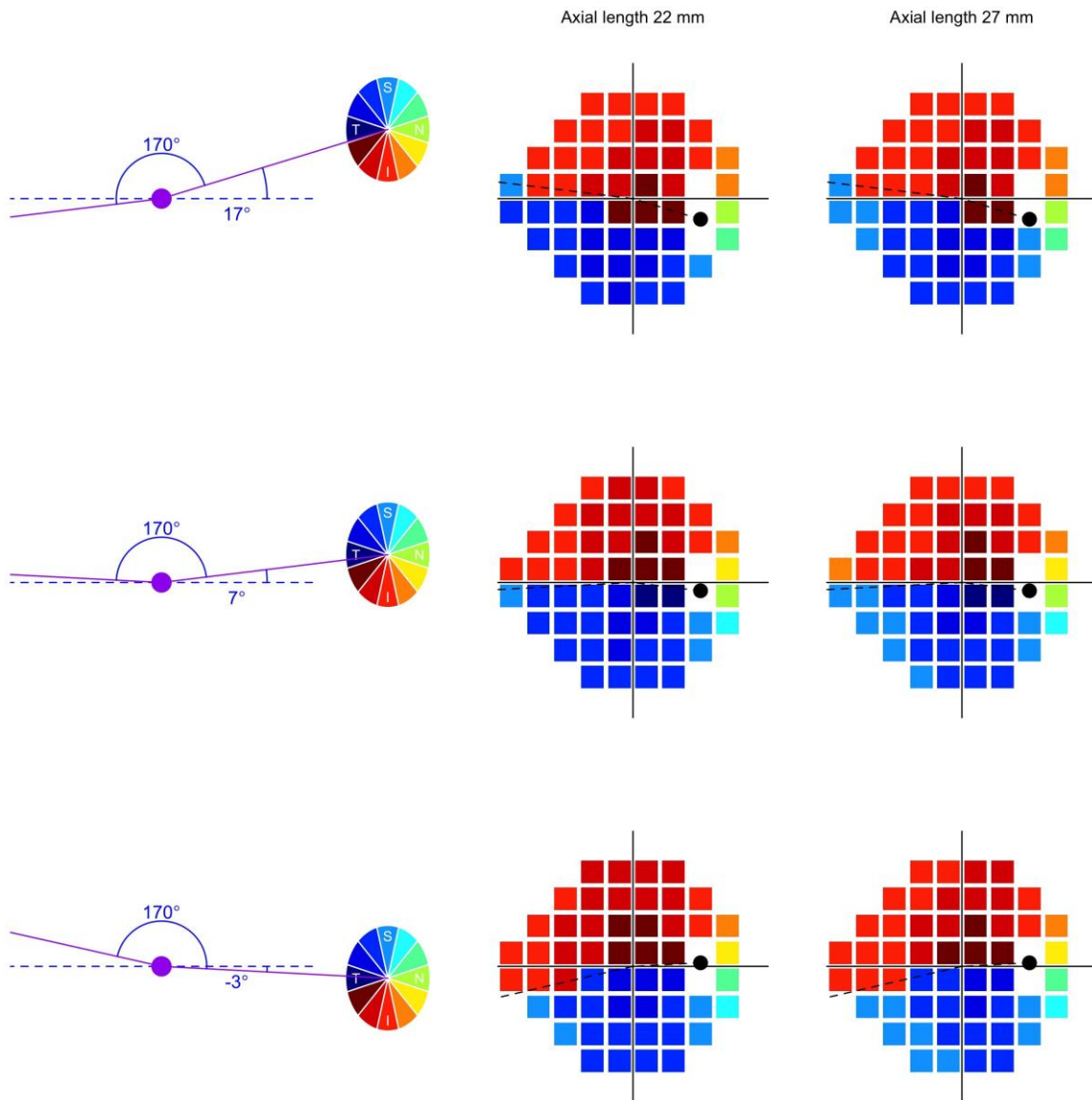
121 factors that result in such a situation. The purpose of our analysis was to determine who might benefit
122 from customised structure-function mapping in a clinical setting.

123

124 **Methods**

125 We have previously developed and described a computational model that outputs a customised map
126 from sectors on the ONH to locations in the visual field given input biometric parameters (distance of
127 the ONH centre from the fovea in horizontal and vertical directions, axial length, position of the
128 temporal raphe).^{4, 5, 22} Our model provides mapping from any location (in x,y coordinates) in the
129 visual field to a resolution of 1 degree of angle on the ONH. For the purposes of the analysis
130 described herein, we restrict our mapping to the visual field locations included in the 24-2 pattern
131 (Humphrey Field Analyzer, Carl Zeiss Meditec, Dublin CA, USA).

132 Some graphical examples of the maps produced by our model are shown in Figure 1. In this example,
133 the horizontal displacement of the ONH relative to the fovea is kept fixed, while the vertical
134 displacement varies. The temporal raphe is fixed at 170 degrees from the angle between the fovea and
135 the optic disc (FoDi) angle because the limited data available from high resolution imaging of the
136 temporal raphe is consistent with this average value.^{15, 16} The effect of changing axial length is also
137 illustrated.



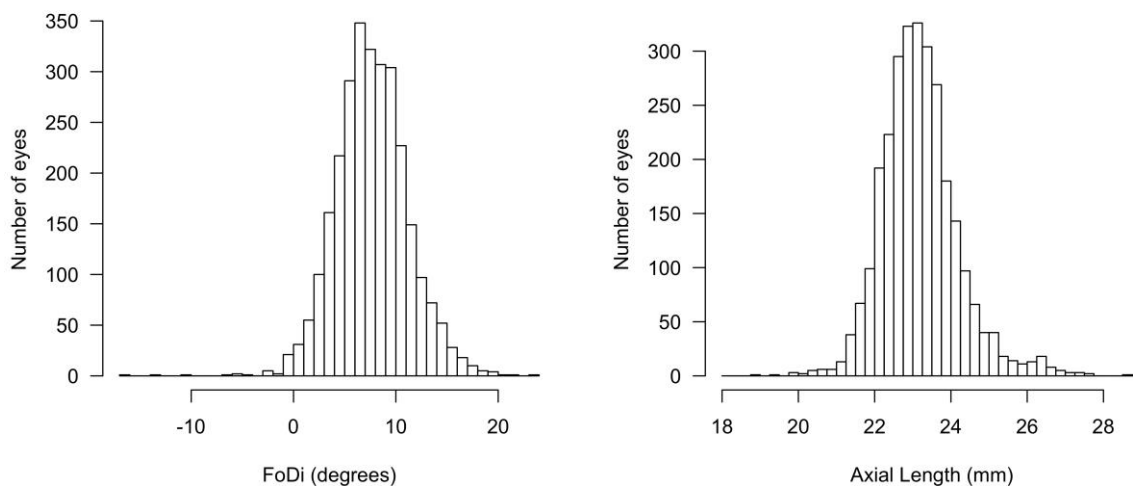
138

139 **Figure 1:** Schematic illustration of customised mapping from 30 degree sectors of the optic nerve
 140 head to the 24-2 locations in visual field space in right eye format. The left hand side shows three
 141 different positions of the optic nerve relative to the fovea. Corresponding maps for both shorter and
 142 longer axial lengths are illustrated on the right hand side.

143 Including all plausible anatomical variants of the parameters that input into the model results in over
 144 11550 maps.⁴ However some of these are much more frequent than others. In order to explore the
 145 expected frequency of “atypical” mapping, we used data from 2836 eyes from the Beijing Eye Study.
 146 The Beijing Eye Study 2011 was a population-based cross-sectional survey performed in an urban

147 region and a rural region of Beijing in Northern China and included adults with an age of over 50
148 years. It has been described in detail previously.^{14, 23, 24} The Beijing Eye Study received human
149 research ethics approval from the Medical Ethics Committee of the Beijing Tongren Hospital and all
150 participants gave informed written consent. For this study we used the following information from
151 each eye: axial length, distance of the centre of the optic nerve head from the fovea in both horizontal
152 and vertical dimensions as derived from retinal photography using fundus camera Type CR6-45NM;
153 Canon Inc., Tokyo, Japan (for further details of the procedure to derive the optic nerve position
154 see:¹⁴) For all analyses we assumed that the position of the temporal raphe was 170 degrees from the
155 angle between the fovea and disc (FoDi angle) as illustrated in Figure 1, as the position of the raphe
156 was not individually measured in the Beijing Eye Study and previous studies suggest an angle of
157 approximately 170 degrees on average.^{15, 16} In order to project the ONH position onto a blind spot
158 position on the visual field, we assumed a nodal point that was 17.2 mm for an eye with axial length
159 22.2mm,²⁵ and scaled it directly with axial length. The data included significant population variance
160 in axial length and in the angle of the ONH from the fovea (Figure 2), as well as the distance from the
161 fovea in x, y coordinates.

162



163

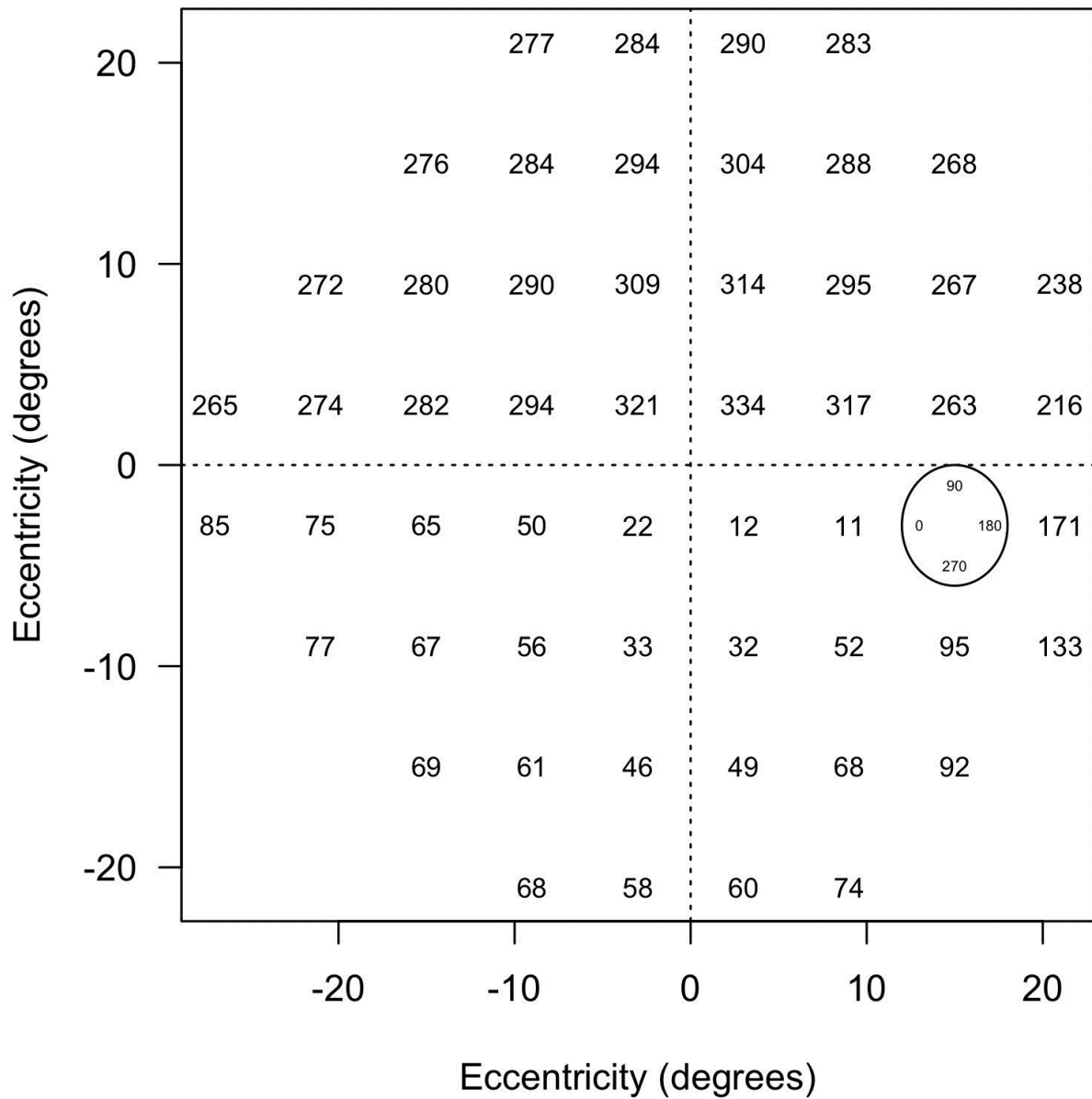
164 **Figure 2:** A) *Distribution of axial lengths within the population database; B) Distribution of angles*
165 *between the fovea and the optic disc (FoDi) within the population. The sign of the FoDi angle is as*
166 *per the schematic illustration in Figure 1.*

167

168

169 **Analysis**

170 Our baseline condition is the map for the “average eye” within the Beijing Eye study dataset (axial
171 length 23.23mm, FoDi angle 7.672 degrees, distance from fovea to ONH centre 4.68mm), as
172 illustrated in Figure 3. To determine the “average eye” in the data set we first computed the mean of
173 each of three parameters: axial length (23.19mm), fovea-disc angle (7.68 degrees), and fovea-disc
174 distance (4.77mm) the hypotenuse of fovea-disc in the horizontal and vertical dimensions) over the
175 whole data set. To ensure that we had an anatomically plausible combination of the three parameters,
176 we then selected the eye in the data set that had the smallest sum-of-squared distance from these three
177 mean values to be the average. The average map in Figure 3 is similar to other published mapping
178 schema that have been derived as the “best fit” from a population of eyes.^{1,3}



179

180 **Figure 3:** The structure to function map for the average eye. Each location in visual field space from
 181 the 24-2 test pattern is represented. The number at each test location is the estimated angle of
 182 insertion (in degrees) of the retinal nerve fibers into the ONH that correspond to the specific location
 183 in visual space.

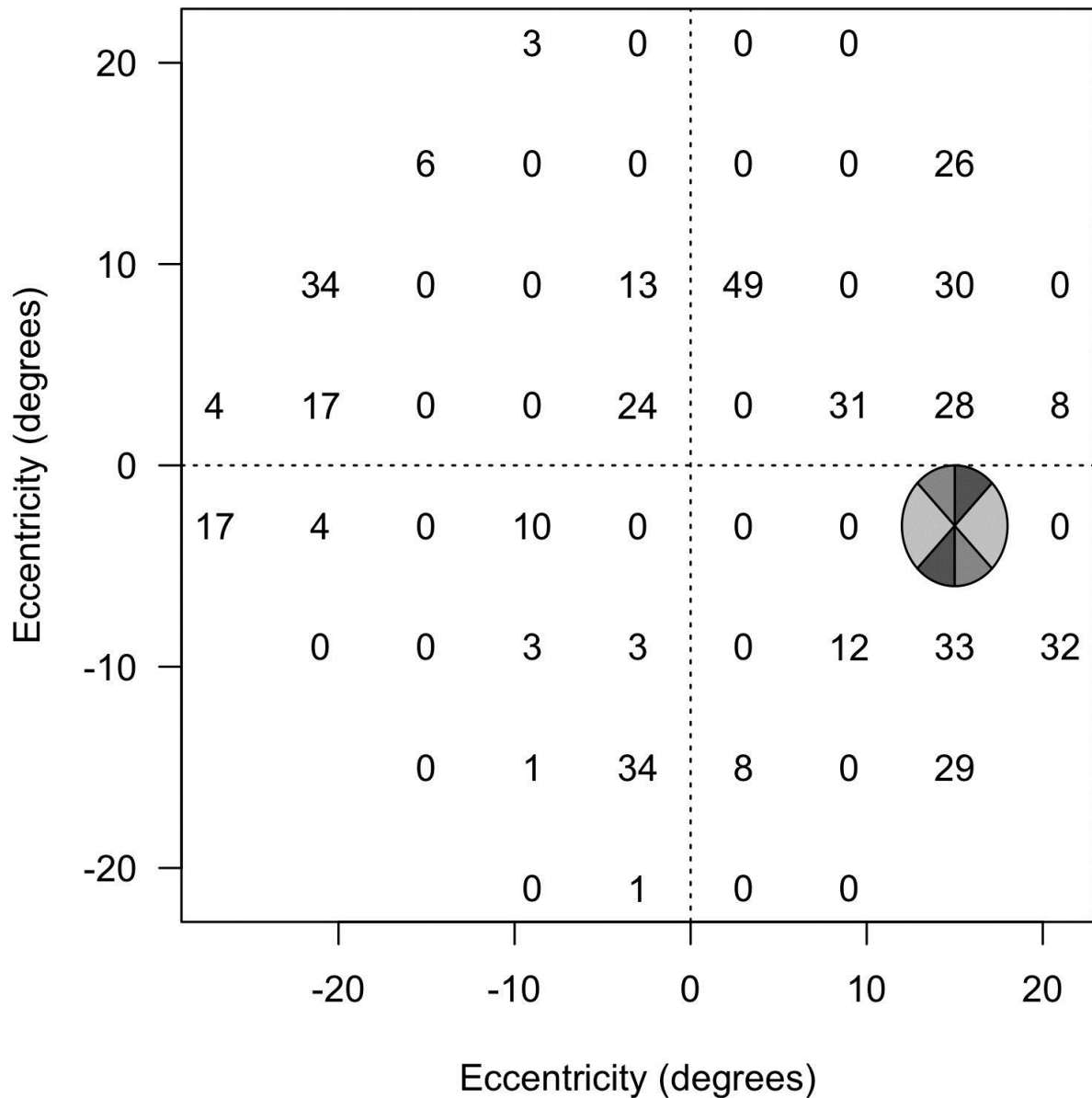
184

185 In order to quantify the difference between using an individualised map versus the average-eye map,
 186 we report the following two items for each location in the 24-2 test pattern.

- 187 1) The proportion of eyes where at least one visual field location moved to a different sector
188 within a predefined division of the ONH into 6 large sectors. Large sector maps are in
189 common usage in current clinical instrumentation, principally derived from the mapping
190 schema reported by Garway-Heath et al²⁶.
- 191 2) The proportion of eyes where the mapped point on the ONH was more than 15 degrees, 30
192 degrees or 60 degrees away from the insertion point for the same location in the eye with the
193 population average anatomy.

194 **Results**

195 Figure 4 shows the percentage of eyes where each individual 24-2 visual field location mapped to a
196 different ONH sector than described for the average eye using the six large ONH sectors in common
197 clinical use.



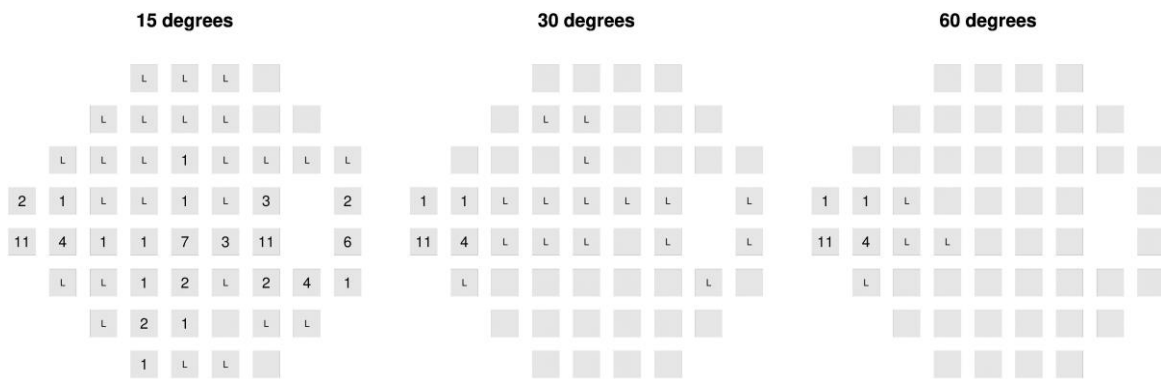
198

199 **Figure 4:** For each 24-2 visual field location, the percentage of eyes in the population database that
 200 fall into a different ONH sector than that of the average eye. The ONH is divided into the 6 sectors of
 201 the Garway-Heath map²⁶ (as illustrated) at the blind spot in the visual field at (-15, -2) for a right eye.

202

203 Figure 5 shows the percentage of eyes that deviated from the average-eye map by more than 15
 204 degrees, 30 degrees or 60 degrees, for each location in the visual field. For the more than 60 degree
 205 case, in all eyes, the locations mapped to the opposite pole of the ONH than conventionally

206 considered (as per Figure 1 upper and lower panel). A total of 12% of individuals showed this pattern
207 of results.

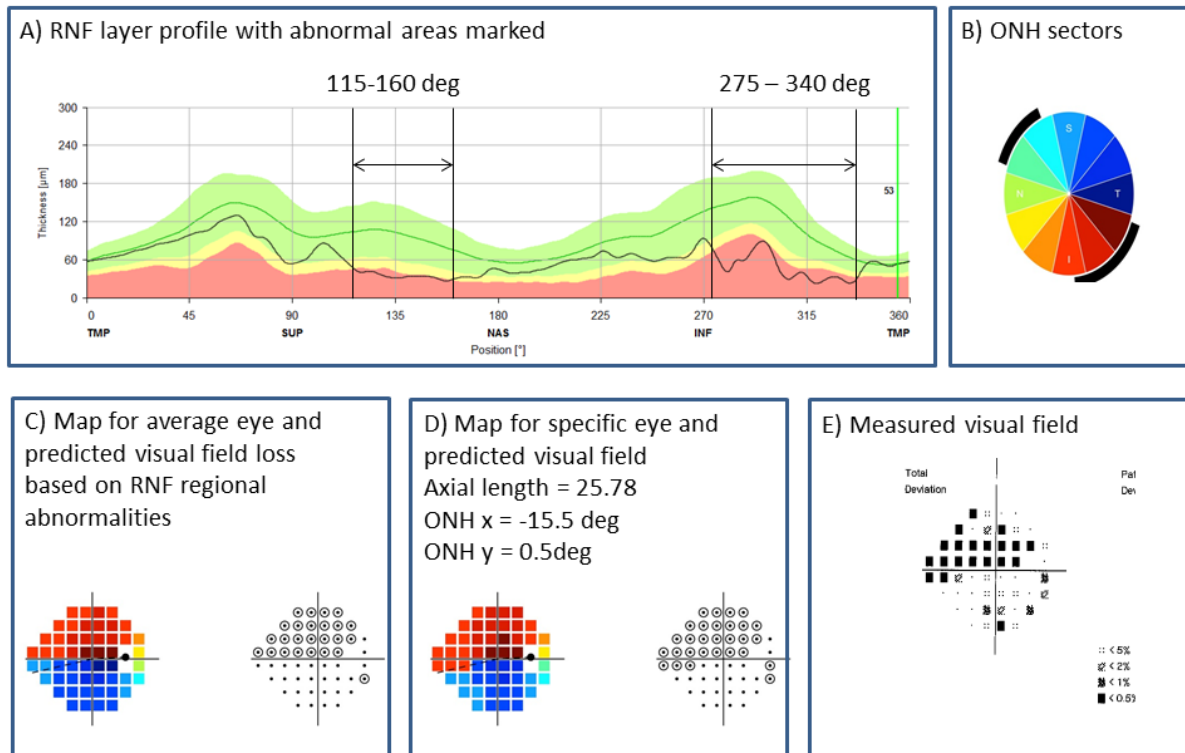


208

209 **Figure 5:** For each location in the visual field, the percentage of eyes where the mapped location for
210 the individualised structure-function map deviated from the average-eye map by more than 15
211 degrees (left panel), 30 degrees (middle panel) and 60 degrees (right panel). The proportion is
212 represented numerically, with locations where the proportion was larger than 0 but less than 0.5%
213 marked with an L.

214

215 Comparison of Figure 5 to Figure 4 illustrates that many of the eyes that mapped into a different large
216 sector from the average eye (Figure 4) were actually displaced by less than 15 degrees (Figure 5).
217 Shifts of between 15-30 degrees were present largely for visual field locations along the nasal
218 horizontal midline and are mainly driven by variation in the position of the optic nerve head relative
219 to the fovea. Large deviations (greater than 60 degrees) from the average eye were noted in the nasal
220 step region, in particular inferiorly. These arise from non-horizontal positioning of the temporal raphe,
221 which results in the visual field location mapping to the opposite vertical pole of the optic nerve than
222 traditionally assumed by a strictly horizontal raphe (Figure 1).



223

224 **Figure 6:** A primary open angle glaucoma patient case example (right eye) that illustrates departure
 225 from average-eye structure-function mapping. A) a peripapillary RNFL OCT scan with two areas of
 226 abnormal RNFL thinning marked; B) colour code for the division of the ONH into 12 x 30 degree
 227 sectors; C) coloured map for the average eye where the colours for each visual field location indicate
 228 the relevant sector on the ONH in panel B, and the grey scale visual field map marks the expected
 229 locations of visual field damage from the damaged RNFL sectors marked in panel A; D) as per panel
 230 C but for a map customised to the axial length and ONH position of the individual; E) the measured
 231 24-2 visual field damage.

232

233 Figure 6 shows a clinical example of the type of scenario where the mapping is significantly deviated
 234 from average in the nasal step region. Figure 6A shows the OCT RNFL peripapillary scan
 235 (Spectralis, Heidelberg Engineering GmbH, Heidelberg, Germany) for an individual with primary
 236 open angle glaucoma. The RNFL profile shows two sectors of abnormality: between approximately

237 115-160 degrees, and between approximately 275-340 degrees. Panel 6B marks those regions on the
238 ONH sectorial depiction. Panel 6C shows the predicted locations of visual field damage based on the
239 average-eye map. However, this eye is not average and instead has an ONH minimally displaced from
240 the horizontal midline (ONH x = -15.5 deg, ONH y = 0.5deg, fovea to disc angle = -3.1deg; axial
241 length = 25.78mm). Panel 6D shows the predicted locations of visual field damage based on the
242 individual eye's geometric parameters. Panel 6E shows the actual measured visual field for this
243 individual (Humphrey Field Analyser, 24-2 SITA standard).

244

245 **Discussion**

246 Significant anatomical variation exists between individuals for ocular parameters that influence the
247 mapping between common clinical structural measures, and locations in visual space. Such variation
248 is sufficient to result in different maps between locations in visual field space and the ONH. The
249 largest displacement is in the nasal step region of the visual field (temporal retina). Our analysis of the
250 population-based data from the Beijing Eye Study predicts that approximately 12% of people will
251 have markedly altered mapping between structure and function for visual field locations in this area
252 (mapping to the opposite side of the ONH than traditionally assumed – see Figure 5, and
253 schematically in Figure 1). Other smaller areas of displacement also occur, but given the resolution of
254 current clinical analysis of the ONH and the expected pattern of loss in glaucoma, arguably the most
255 clinically significant area of errors in mapping arise for the nasal step region of the visual field.

256

257 While our model can map to 1 degree resolution on the ONH, we have previously shown that
258 measurement error in the various parameters relevant to customised mapping (position of the ONH,
259 axial length) produces a practical sector limit of approximately 30 degrees for clinical use.⁹ Most
260 current clinical mapping schema include wider sector boundaries than 30 degrees. Improved precision
261 of customised mapping should enable more anatomically localised linking of data from structure to

262 function. It remains to be seen whether more localised mapping results in better ability to monitor
263 combined change in structural and functional parameters in glaucoma, however, it is likely that when
264 smaller ONH sectors are used to enhance the spatial resolution of mapping the importance of
265 personalising the maps will increase as fewer patients will fit within the “average” template since
266 small deviations from average will be more likely to result in changes in mapped ONH sector (Figure
267 5). Similar to our current study however, the importance of personalising structure-function mapping
268 in monitoring spatially localised progression will be best assessed through analysis of individual eyes
269 with non-average anatomical parameters, rather than by comparison of population metrics.

270 Advances in OCT technology have resulted in ocular imaging being used very routinely in glaucoma
271 management. The anatomical parameters that are required for custom mapping are macro-features (in
272 particular, the position of the ONH relative to the fovea) so do not necessary require OCT to acquire,
273 but are now exported routinely with several commercial OCT systems. Hence, incorporating a more
274 customised approach to structure-function mapping should be relatively simple. An exception is the
275 determination on an individual basis of the positioning of the temporal raphe, which currently requires
276 custom high resolution imaging to accurately measure. For this reason, the absence of individual data
277 regarding the positioning of the temporal raphe is a limitation of this study. We make the simplifying
278 assumption that the temporal raphe is typically positioned at an angle of 170 degrees from the fovea-
279 disc angle (see Figure 1). Available evidence suggests that this assumption is reasonable “on-
280 average”, however, given that we are specifically interested in the non-average eye, there will be
281 cases where this relationship does not hold. Indeed, inspection of the data from the 15 eyes presented
282 in Chauhan et al,¹⁵ suggests some significant variation around the approximate average of 170 degrees
283 from the fovea-disc angle. With only 15 eyes, however, it is not possible to derive a predictive
284 relationship between the parameters that were measured in the Beijing data, and the position of the
285 raphe (if, indeed, there is such a relationship). Clearly, further refinement of the predictions made by
286 our analysis will be possible if a large database with all of axial length, fovea-disc angle and
287 individually measured temporal raphe is available in the future.

288 We estimated the temporal raphe at 170 degrees from the fovea-disc angle based on previous
289 literature,¹⁵ and it is clear that in a significant proportion of eyes, the temporal raphe is not strictly
290 horizontal. Here, we only present mapping data for the 24-2 visual field pattern (6 degree spacing,
291 across the central +/- 24 degrees of visual field). Non-horizontal positioning of the temporal raphe is
292 also predicted to significantly alter the mapping for the 10-2 visual field pattern, which covers a
293 smaller visual eccentricity, but presents data closer to the horizontal midline, in addition to other
294 commonly used patterns that place points close to the horizontal midline (eg the G-pattern in the
295 Octopus perimeter). The model used to customise mapping between visual field locations and sectors
296 on the optic nerve head within this study uses a few simple input parameters (axial length, x-y
297 distance of the fovea from the optic nerve head, position of the temporal raphe), as these are
298 considered major, macro-anatomical features that are likely to significantly alter the anatomical
299 trajectories for retinal nerve fibre bundles from the retinal periphery to their point of insertion on the
300 ONH. Other retinal features may be important for structure-function mapping, such as the position of
301 the major retinal blood vessels,²⁷ or individual differences in retinal ganglion cell numbers and density
302 across the retina, or individual differences in the shape of the macular region.^{10, 28} Such features were
303 not included in this study. Future work may refine the features that contribute to localised differences
304 in structure to function mapping, however, we expect that major, clinically significant, differences
305 between individuals (for example, complete swapping in mapping from inferior to superior
306 hemifields) will be primarily driven by macro features such as the positioning of the raphe, and hence
307 are encapsulated herein.

308 In this study, we chose to use the average eye from within our database as the comparison for analysis
309 rather than an established structure-function map. Our average map is similar to the map of Garway-
310 Heath²⁶ with one exception. The visual field locations superior nasal and inferior nasal to the blind
311 spot take a more linear path in our model than the Garway-Heath population average map. It is worth
312 noting that the map of Garway-Heath was derived from averages across the population for each
313 location in the 24-2 visual field space, hence it is possible that no eyes within the dataset used to
314 construct the map actually conformed to the derived average map for all visual field locations.

315 Furthermore, the Garway-Heath map was derived from a substantially different ethnic demographic
316 than the population of eyes included here (69 eyes from the United Kingdom versus 2836 eyes from
317 China). Consequently, we decided that comparison to our average modelled eye was a fair
318 exploration of the effects of varying local anatomical parameters and likely to lead to more
319 conservative estimates than comparing to a schema derived in a different population.

320

321 Individualised mapping between structure and function could potentially be utilised clinically in
322 several ways. For example, localised structural damage could be used to seed visual field test
323 algorithms^{29,30} or could prompt the targeting of specific localised areas of the visual field for denser
324 sampling or resampling to ensure that more reliable estimates of performance are obtained in key
325 areas of clinical interest. Alternately, new analysis methods that combine probabilities of progression
326 from visual field and imaging data³¹ could be applied on a localised scale. For the average-eye,
327 reasonable assumptions could be made for such analysis from a population average mapping schema,
328 however, our analysis here shows that for a small proportion of eyes an individualised approach is
329 necessary to avoid gross mistakes in mapping.

330 **Conclusions**

331 Population variance in the position of the optic nerve head , axial length and the location of the
332 temporal raphe, predict that individual mapping between visual field locations and sectors on the optic
333 nerve head may be clinically useful. We show that anatomically customised mapping shifts the map
334 markedly in approximately 12% of the general population in the nasal step region where visual field
335 locations can map to the opposite pole of the optic nerve head than traditionally considered.

336

337 **References**

- 338 1. Jansonius NM, Schiefer J, Nevalainen J, Paetzold J, Schiefer U. A mathematical model for
339 describing the retinal nerve fiber bundle trajectories in the human eye: average course,
340 variability, and influence of refraction, optic disc size and optic disc position. *Exp Eye Res.*
341 2012;105:70-8.
- 342 2. Lamperter J, Russell RA, Zhu H, Asaoka R, Yamashita T, Ho T, et al. The influence of
343 intersubject variability in ocular anatomical variables on the mapping of retinal locations to the
344 retinal nerve fiber layer and optic nerve head. *Invest Ophthalmol Vis Sci.* 2013;54(9):6074-82.
- 345 3. Garway-Heath DF, Poinoosawmy D, Fitzke FW, Hitchings RA. Mapping the visual field to the
346 optic disc in normal tension glaucoma eyes. *Ophthalmology.* 2000;107(10):1809-15.
- 347 4. Denniss J, McKendrick AM, Turpin A. An anatomically-customisable computational model
348 relating the visual field to the optic nerve head in individual eyes. *Invest Ophthalmol Vis Sci.*
349 2012;53(11):6981-90.
- 350 5. Turpin A, Sampson GP, McKendrick AM. Combining ganglion cell topology and data of
351 patients with glaucoma to determine a structure-function map. *Invest Ophthalmol Vis Sci.*
352 2009;50(7):3249-56.
- 353 6. Carreras FJ, Rica R, Delgado AV. Modeling the patterns of visual field loss in glaucoma.
354 *Optom Vision Sci.* 2011;88(1):63-79.
- 355 7. Gardiner SK, Johnson CA, Cioffi GA. Evaluation of the structure-function relationship in
356 glaucoma. *Invest Ophthalmol Vis Sci.* 2005;46:3712-7.
- 357 8. Ferreras A, Pablo LE, Garway-Heath DF, Fogagnolo P, Garcia-Feijoo J. Mapping standard
358 automated perimetry to the peripapillary retinal nerve fiber layer in glaucoma. *Invest*
359 *Ophthalmol Vis Sci.* 2008;49(7):3018-25.
- 360 9. Denniss J, Turpin A, McKendrick AM. Individualised structure-function mapping for
361 glaucoma: practical constraints on map resolution of clinical and research applications. *Invest*
362 *Ophthalmol Vis Sci.* 2014;55(3):1985-93.
- 363 10. Turpin A, Chen S, Sepulveda JA, McKendrick AM. Customising structure-function
364 displacements in the macula for individual differences. *Invest Ophthalmol Vis Sci.*
365 2015;56(10):5984-9.
- 366 11. Hood DC, Nguyen M, Ehrlich AC, Raza AS, Sliesoraityte I, De Moraes CG, et al. A test of a
367 model of glaucomatous damage of the macula with high-density perimetry: Implications for the
368 locations of visual field test points. *Transl Vis Sci Technol.* 2014;3(3):5. e collection 2014.
- 369 12. Atchison DA, Jones CE, Schmid KL, Pritchard N, Pope JM, Strugnell WE, et al. Eye shape in
370 emmetropia and myopia. *Invest Ophthalmol Vis Sci.* 2004;45:3380-6.
- 371 13. Chauhan BC, Burgoyne CF. From Clinical Examination of the Optic Disc to Clinical
372 Assessment of the Optic Nerve Head: A Paradigm Change. *Am J Ophthalmol.* 2013;156:218-
373 27.
- 374 14. Jonas RA, Wang YX, Yang H, Li JJ, Xu L, Panda-Jonas D, et al. Optic disc - fovea angle: The
375 Beijing Eye Study 2011. *PLoS One.* 2015;10(11):e0141771.
- 376 15. Chauhan BC, Sharpe GA, Hutchinson DM. Imaging of the temporal raphe with optical
377 coherence tomography. *Ophthalmology.* 2014;121(11):2287-8.
- 378 16. Tanabe F, Matsumoto C, Okuyama S, Takada S, Numata T, Kayazawa T, et al. Imaging of
379 temporal retinal nerve fiber trajectory with Transverse Section Analysis. *IOVS ARVO Annual*
380 *Meeting Abstract.* 2014;55(13):957.
- 381 17. Huang G, Luo T, Gast TJ, Burns SA, Malinovsky VE, Swanson WH. Imaging glaucomatous
382 damage across the temporal raphe. *Invest Ophthalmol Vis Sci.* 2015;56(6):3496-504.
- 383 18. Amini N, Nowroozizadeh S, Cirineo N, Henry S, Chang T, Chou T, et al. Influence of the disc-
384 fovea angle on limits of RNFL variability and glaucoma discrimination. *Invest Ophthalmol Vis*
385 *Sci.* 2014;55:7332-42.
- 386 19. Asman P, Heijl A. Glaucoma Hemifield Test. Automated visual field evaluation. *Arch*
387 *Ophthalmol.* 1992;110(6):812-9.
- 388 20. Ganeshrao SB, Turpin A, Denniss J, McKendrick AM. Enhancing structure-function
389 correlations in glaucoma with customised spatial mapping. *Ophthalmology.* 2015;122(8):1695-
390 705.
- 391 21. Danthurebandara VM, Sharpe GP, Hutchison DM, Denniss J, Nicoleta MT, McKendrick AM,
392 et al. Enhanced structure-function relationship in glaucoma with an anatomically and

393 geometrically accurate neuroretinal rim measurement. *Invest Ophthalmol Vis Sci.* 2014;56:98-
394 105.

395 22. Denniss J, Turpin A, Tanabe F, Matsumoto C, McKendrick AM. Structure-function mapping:
396 variability and conviction in tracing retinal nerve fiber bundles and comparison to a
397 computational model. *Invest Ophthalmol Vis Sci.* 2014;55(2):728-236.

398 23. Jonas RA, Wang YX, Yang H, Li JJ, Xu L, Panda-Jonas D, et al. Optic disc-fovea distance,
399 axial length and parapapillary zones. *The Beijing Eye Study. PLoS One.* 2015;10(9):e0138701.

400 24. Wang YX, Xu L, Yang H, Jonas JB. Prevalence of glaucoma in North China: The Beijing Eye
401 Study. *Am J Ophthalmol.* 2010;150:917-24.

402 25. Gullstrand A. *Helmholtz's Physiological Optics.* Optical Society of America. 1924;New
403 York(Appendix):350-8.

404 26. Garway-Heath DF, Holder GE, Fitzke FW, Hitchings RA. Relationship between
405 electrophysiological, psychophysical, and anatomical measurements in glaucoma. *Invest*
406 *Ophthalmol Vis Sci.* 2002;43(7):2213-20.

407 27. Fujino Y, Yamashita T, Murata H, Asaoka R. Adjusting circumpapillary retinal nerve fiber
408 layer profile using retinal artery position improves the structure-function relationship in
409 glaucoma. *Invest Ophthalmol Vis Sci.* 2016;57:3152-8.

410 28. Sepulveda JA, Turpin A, McKendrick AM. Individual differences in foveal shape: feasibility of
411 individual maps between structure and function within the macular region. *Invest Ophthalmol*
412 *Vis Sci.* 2016;57(11):4772-8.

413 29. Denniss J, McKendrick AM, Turpin A. Towards patient-tailored perimetry: Automated
414 perimetry can be improved by seeding procedures with patient-specific structural information.
415 *Trans Vis Sci and Tech.* 2013;2(4):1-13.

416 30. Ganeshrao SB, McKendrick AM, Denniss J, Turpin A. A Perimetric Test Procedure that Uses
417 Structural Information. *Optom Vis Sci.* 2015;92(1):70-82.

418 31. Russell RA, Malik R, Chauhan BC, Crabb DP, Garway-Heath DF. Improved estimates of
419 visual field progression using Bayesian linear regression to integrate structural information in
420 patients with ocular hypertension. *Invest Ophthalmol Vis Sci.* 2012;53(6):2760-9.

421

422

423

424

425